A&A 393, 991–996 (2002)
DOI: 10.1051/0004-6361:20021092

Astronomy & Astrophysics

Wavelet analysis of instability-generated line profile variations in hot-star winds

L. Dessart[1] and S. P. Owocki[2]

[1] N&S Sterrenkunde Universiteit Utrecht, Princetonplein 5, 3584 CC Utrecht, The Netherlands
e-mail: l.dessart@phys.uu.nl
[2] Bartol Research Institute of the University of Delaware, Newark, DE 19716, USA
e-mail: owocki@bartol.udel.edu

Accepted 21 May 2002 / Received 23 July 2002

Abstract. We investigate whether instability-generated structure of line-driven stellar winds can account for the emission line profile variability (LPV) observed in hot star spectra. In a previous paper, we introduced a three-dimensional (3D) "patch" method to compute the temporal evolution of the wind emissivity, based on 1D radiation hydrodynamics simulations. Here we apply a wavelet analysis to these *synthetic* LPVs, allowing a direct comparison with observations analysed in the same way, with particular focus on the characteristic velocity scale of LPVs at various frequency locations within the line profile. Wavelet analyses of observed LPV generally show this scale to *increase* from 50 to 100–200 km s^{-1} from line-centre to edge. We argue here that the characteristic sub-peak broadening is dominated at line-centre by the lateral spatial extent of wind structures, while at line-edge it is controlled by their intrinsic radial velocity dispersion. We find that the wavelet transforms of synthetic LPV yield characteristic widths that are comparable to observed values at line-centre, but much narrower at line-edges. We thus conclude that the patch size of 3 deg assumed here provides a reasonable representation of the lateral coherence length associated with observed LPV, but that the 1D instability models that form the basis of the patch method have too low a radial velocity dispersion to reproduce the characteristic widths observed at line edge. We discuss how the latter limitation might be overcome by inclusion of radial velocity shear, and also outline possible approaches to developing multi-dimensional instability simulations that could account for such shear effects.

Key words. line: formation – radiative transfer – stars: atmospheres – stars: early-type – stars: mass-loss

1. Introduction

Hot, luminous stars are characterised by dense outflows ($\dot{M} \sim 10^{-5}\ M_\odot\ \mathrm{yr}^{-1}$) and large asymptotic velocities ($v_\infty \sim 1000$ km s^{-1}). The engine at the origin of such winds is believed to be the scattering of continuum light by optically thick lines of metals. Although the theory of radiatively driven winds is in many ways quite successful (Castor et al. 1975, hereafter CAK; Pauldrach et al. 1986), a variety of phenomena remain poorly understood, such as X-ray production and spectroscopic variability.

In particular, the emission LPV observed in hot-star spectra has been the subject of many phenomenological investigations (Robert 1992; Lépine & Moffat 1999, hereafter LM). For example, LM described the LPV as resulting from the cumulative sum of a large number of Discrete Wind Emission Elements (DWEEs), with adjustable velocity and intensity properties. While informative, this characterisation still leaves considerable uncertainty about the physical nature and dynamical origin of the underlying wind structure that might give rise to such DWEEs. The overall goal of this and related studies in this series is to examine how well such LPV can be understood as stemming from flow structure that arises dynamically from intrinsically strong instabilities associated with the radiative driving of such winds.

We base our approach on radiation hydrodynamics simulations of the instability intrinsic to line driving (Owocki et al. 1988). Numerous simulations using several independent hydrodynamical codes (Owocki 1991; Feldmeier 1995; Dessart & Owocki 2002a, hereafter DO) have typically yielded a similar overall structure, characterised by radially extended, high-speed, rarefied regions that separate narrow, slow, compressed, dense clumps. Despite this apparently extensive structure, when viewed in terms of the variation of velocity vs. a *mass* distribution coordinate, the bulk of wind mass actually follows closely the velocity law for the standard, steady-state CAK model (Fig. 1). Moreover, because of the computational expense of evaluating the non-local integral expressions for the line-driving force, such instability simulations have all (except for the experimental approach introduced by Owocki 1999) been limited to 1D descriptions of just the *radial* flow structure, thus ignoring the *lateral* flow and variations that would be expected in more realistic 2D or 3D models. Nonetheless, the first paper of this series (DO) introduced a "3D patch method"

Send offprint requests to: L. Dessart,
e-mail: l.dessart@phys.uu.nl

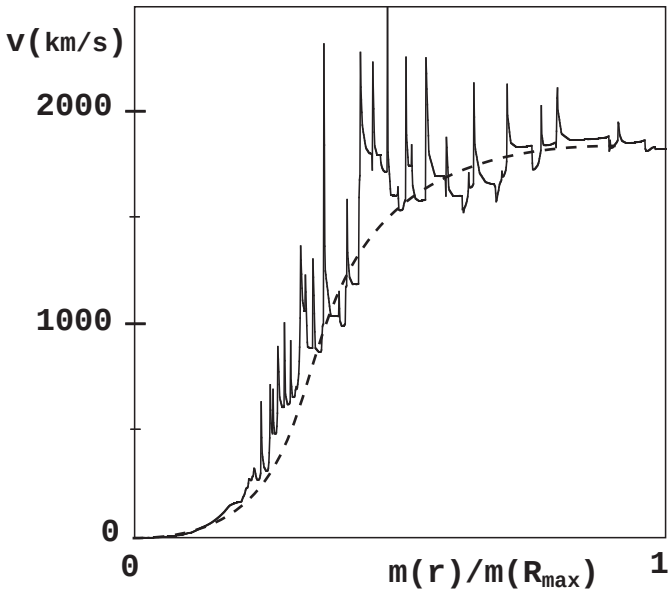

Fig. 1. (Solid) Snapshot of the velocity $v(r)$ as a function of the cumulative mass $m(r)$ defined as $m(r) = \int_{R_\star}^{r} 4\pi a^2 \rho(a) \mathrm{d}a$. The "unstable" form of the radiative force is added to the momentum equation in the hydrodynamics simulations. Notice how the velocity jumps correspond to narrow mass jumps. The outermost point in the simulation is $R_{\max} = 10R_\star$. **(Dashed)** id. but for a calculation with the "stable" form of the radiation force, as described by CAK.

for using such 1D simulations to generate synthetic line emission spectra, and showed that, with proper choice of "patch size" (about 3 deg), the resulting synthetic LPV have a fluctuation amplitude and general morphology that seem *qualitatively* quite similar to observed LPV.

In the present paper, we now apply more *quantitative, objective* measures for comparing these observed and synthetic LPVs, based in particular on the "wavelet transform" analysis (Sect. 2) that has been used extensively to characterise observed LPV (Lépine 1998; Lépine et al. 1996; LM). We focus in particular (Sect. 3) on the inferred velocity width of the associated structure and how this varies with wavelength position within the line profile. We find that, while the dynamical models reproduce roughly the observed velocity width at line-centre, they yield velocity structure that is much narrower than observed in the line wings. We examine (Sect. 4) the effect of varying the assumed patch size, showing that this influences mainly the inferred velocity width at line-centre, and thus cannot generally resolve the discrepancy in the line wings. We discuss (Sect. 5) how this discrepancy likely stems from the low level of radial velocity dispersion of wind structures that seems quite intrinsic to 1D simulation models. Finally, we conclude (Sect. 6) with an outline for carrying out future 2D and 3D simulations that could allow a level of radial velocity shear needed to reproduce the observed velocity widths in the line wings.

2. Characteristics of observed micro-variability

Let us begin with an overview of the wavelet analysis, developed originally by LM to provide a quantitative statistical characterisation of observed LPV, but applied here to obtain analogous and thus comparable statistical measures for the synthetic spectra obtained from our hydrodynamical simulations.

The observations presented in LM describe the observed LPV of the strongest un-blended optical emission line in a sample of WR stars. Observations are one in-hour integrations, with a resolution of 10 km $s^{-1}$and a signal of 100 typically, and have concentrated usually on one line only (He II 5411 Å for nitrogen WR stars, C III 5696 for carbon WR stars, and He II 4686 Å for O supergiants). The fundamental common property of LPV in all observed stars is the presence of sub-peaks that deviate from the mean profile flux, which migrate towards the nearer line-edge in a few hours. Such sub-peaks possess a velocity width, markedly different across the profile. This characteristic scale is believed to represent a key property of wind structures which deserves quantitative scrutiny, suited for a wavelet analysis.

For both actual and synthetic spectra, the basic quantity to analyse is the line profile emissivity $F(\xi, t)$, where ξ is a given wavelength measured in velocity units from line-centre, i.e. $\xi = (\lambda/\lambda_0 - 1)c/v_\infty$. For N such profiles, one can define the time average profile over the whole dataset, $< F(\xi, t) >_{\mathrm{t}}$, and from this calculate the residual as

$$R(\xi, t) = F(\xi, t) - < F(\xi, t) >_{\mathrm{t}} .$$

The principle of the Wavelet Power Spectrum (WPS) method, as first applied to emission lines of hot star spectra by Lépine (1998), is to compute the wavelet transform by convolving these residuals with a basis function Φ, the argument of which is a relative velocity position $\xi - \xi'$ scaled by a characteristic velocity width σ_ξ,

$$\tilde{R}(\xi, \sigma_\xi, t) = \int_{-\infty}^{\infty} R(\xi', t)\Phi((\xi - \xi')/\sigma_\xi)\mathrm{d}\xi'/\sigma_\xi.$$

A commonly chosen basis is the so-called "Mexican-hat" function,

$$\Phi(\xi) = (1 - \xi^2)\exp(-\xi^2/2),$$

with the convenient properties $\Phi(0) = 1$ and

$$\int_{-\infty}^{\infty} \Phi(\xi)\mathrm{d}\xi = 0.$$

Carrying out an average over all wavelet transforms in the time series provides a more representative description of the sub-peak scales typically present at ξ, one that is less sensitive to special (short-lived) outflow events. For N such individual wavelet transforms, we compute a mean square magnitude

$$< \tilde{R}(\xi, \sigma_\xi) >^2 = \frac{1}{N}\sum_{i=1}^{N} \tilde{R}(\xi, \sigma_\xi, t_i)^2.$$

We also find it instructive to plot selective cuts of this mean wavelet transform over a selected range of profile frequencies $[\xi_1, \xi_2]$,

$$\tilde{R}^2(\sigma_\xi)_{[\xi_1,\xi_2]} = \frac{1}{\xi_2 - \xi_1}\int_{\xi_1}^{\xi_2} < \tilde{R}(\xi, \sigma_\xi) >^2 \mathrm{d}\xi.$$

This is particularly useful when, as is the case here, the wavelet transform is not uniform throughout the profile. In practice,

the change of properties of the wavelet transform are not too sharp, so in our computations, we take a rather broad band width of 400 km s^{-1} (about a quarter of the terminal velocity). Also, observationally, no fundamental variability difference between the two sides of the line profile has been identified so when carrying out such averages, we also form a mean of the transform over the red and blue-side intervals $[\xi_1, \xi_2]$ and $[-\xi_2, -\xi_1]$.

In practice, LM calculated the wavelet transform over all profile frequencies ξ for a range of characteristic velocity scales σ_ξ covering 1–10 000 km s^{-1}. Given the "velocity" resolution at optical wavelengths (few km s^{-1}) and the typical width of line profiles (~1000 km s^{-1}), our WPS calculations are restricted to the range 10–1000 km s^{-1}.

Having defined these mathematical quantities, we can now perform a quantitative assessment of the characteristics of synthetic LPV computed with our patch method.

3. Standard case

For this first case study, we use the wind model of DO, whose characteristics follow roughly the stellar parameters of the canonical O supergiant ζ Puppis. Here, we choose to use the instability simulation method developed by one of us (see Owocki & Puls 1999), implemented within the standard hydrodynamics code VHI (developed by J. Blondin and his colleagues at the University of Virginia). Following the 3D patch synthesis method described by DO, we first prepare the large database of 1D wind layouts used for the cone structure allocation (DO). The specific profiles are derived assuming the wind emission arises over the radial range between 2 and 3 $R_\star$, and with an azimuthal patch size of 3 deg.

The initial analyses of DO indicated that this patch size provides a roughly optimised fit to the overall fluctuation level of observed LPV. We note here that this scale also can be roughly associated with the expected level of lateral acoustic interaction. Specifically, within a characteristic radial flow propagation time R_*/v_∞, lateral pressure interaction propagating at the sound speed a can extend structure over a lateral diameter $2aR_*/v_\infty$. For characteristic sound speed $a \approx 20$ km s^{-1} and wind flow speed $v_\infty \approx 2000$ km s^{-1}, this corresponds to a lateral angle diameter of $\alpha \approx 2a/v_\infty \approx 0.02$ rad ≈1.3 degree, only slightly less than the assumed 3 degree patch size.

We show in Fig. 2 the average profile, the absolute value of the local profile deviation from the mean over all times, the temporal evolution $R(\xi, t)$ of the deviation from the mean, the WPS computed in the manner described in the previous section, and finally four cuts $\tilde{R}(\sigma_\xi)_{[\xi_1,\xi_2]}$ through the WPS sampling the full profile width.

As described in DO, the patch approach is able generally to reproduce the low level observed profile variability, stronger in the flat part region of the profile. One can also identify migrating features that move away from line-centre to the nearest edge. This migration property reflects the acceleration of the underlying wind structures and is at the centre of much controversy. So far, observations suggest very little migration, i.e. small wind acceleration, even for lines thought to form at half the terminal velocity (LM). This seems difficult to reconcile

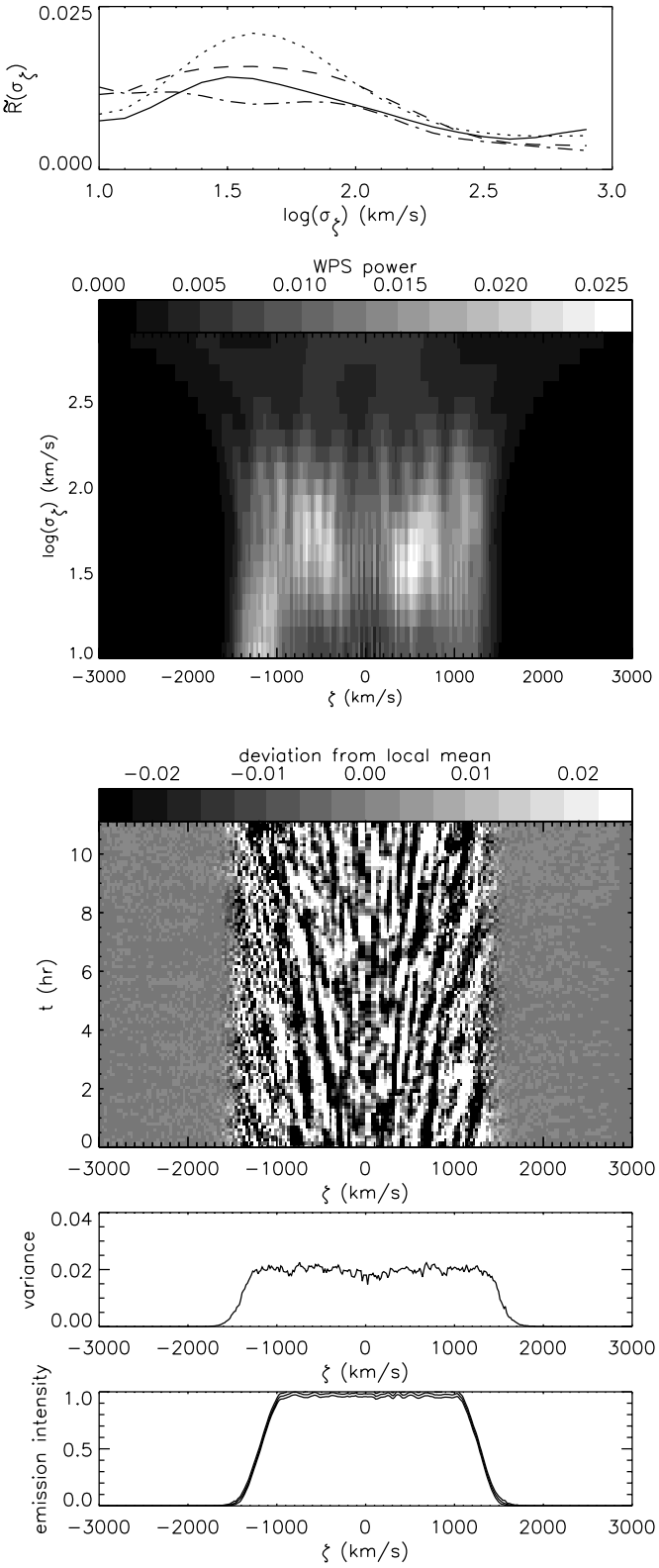

Fig. 2. Series of plots for the 3 deg patch case, with an inner wind line forming region. From bottom to top, we show the average profile, the absolute value of the local profile deviation from the mean (called variance here), the temporal evolution $R(\xi, t)$ of the deviation from the mean, the WPS and finally cuts $\tilde{R}(\sigma_\xi)_{[\xi_1,\xi_2]}$ sampling four regions from line-centre to line-edge. These velocity bands are 1600–1200 km s^{-1} (dashed-dotted line), 1200–800 km s^{-1} (dashed line), 800–400 km s^{-1} (dotted line) and 400–0 km s^{-1} (solid line).

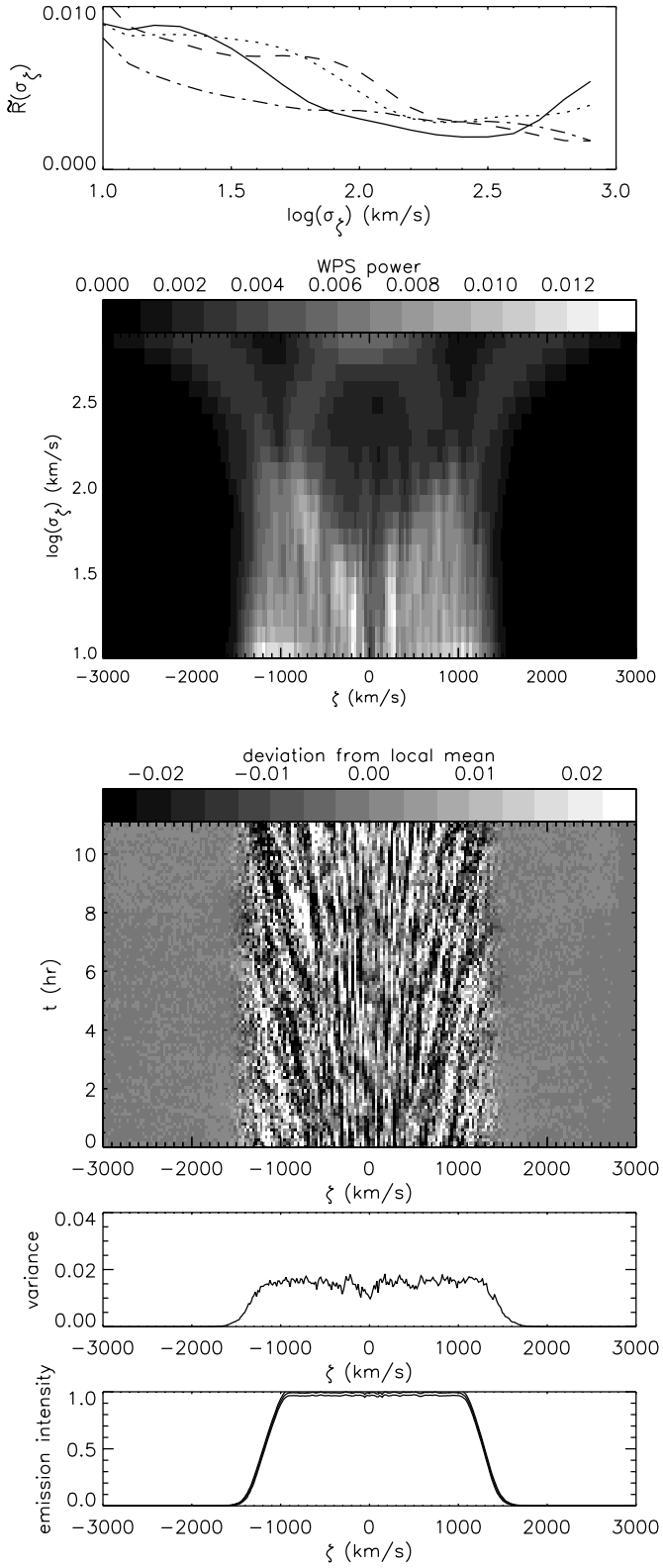

Fig. 3. Same as in Fig. 1, but now for a patch size of only one deg.

with a radiation driving of the wind, the radiation field weakening with height and becoming unable to perform much work beyond a few stellar radii above the photosphere. We will address this and related issues in a future study.

Concentrating here on the computed WPS, we find that the power is not uniform throughout the profile, but, as in observed WPS, shows some distinct structure and trends with velocity position. At line-centre, the power peaks at $\sigma_\xi \sim 50$ km s^{-1}. Moving away from line-centre, at velocity position around $\xi \sim 500$ km s^{-1}, there is initially a further increase in power for somewhat larger velocity widths of $\sigma_\xi \sim 80$ km s^{-1}. But proceeding further toward the line wings, the overall power level falls, with peaks now occurring at much lower width of $\sigma_\xi \sim 30$ km s^{-1}.

These synthetic WPS properties correspond only partly to what is seen in typical observations. The observed WPS do have a comparable power level and width (∼50 km s^{-1}) near line-centre. But quite generally both the power and width are found to increase monotonically away from line-centre, approaching characteristic widths as high as $\sigma_\xi \sim$ 100–200 km s^{-1} at line-edge.

4. Sensitivity of synthetic WPS to choice of parameters

Let us next examine the sensitivity of these dynamical model WPS to assumed parameter values, with particular focus on whether any such models could yield a larger line-edge velocity width that would be in better agreement with observed WPS. For a given star with fixed general stellar and wind parameters (e.g., mass, luminosity, radius, mass loss rate, and wind terminal speed), derivation of LPV within our "3D Patch method" requires three further specifications, namely: 1. patch size, 2. wind location of line-emission, and 3. strength of unstable structure within the 1D dynamical simulation model. We have carried out a broad search varying each of these choices but generally find that in all cases the model WPS still yield line-edge velocity widths that are still substantially narrower than those from observed WPS.

4.1. Patch size

As a specific example, let us first discuss some details of models with various patch sizes. In DO, we showed that increasing the patch size tends to increase the overall profile fluctuation, but with variations near line-centre becoming coherent over a broader wavelength range. Indeed, in the limit of a spherically symmetric structure model, corresponding to a "full-sky patch", the entire profile within a wavelength range corresponding to the velocity of the inner part of the emission region tends to fluctuate in unison. By comparison, the line-edge variation tends to show little velocity coherence, regardless of the patch size.

For smaller patch size, the line-centre fluctuations tend to become narrower, with characteristic velocity width Δv scaling with the patch size α and radial wind speed v as $\Delta v \approx \alpha v$ (DO). Figure 3 show results analogous to those in Fig. 2, but with the patch size reduced from $\alpha = 3$ degrees to $\alpha = 1$ degree. Note in particular that the line-centre velocity width now peaks at a value of about 15 km s^{-1}, about a corresponding factor 3 reduction from the 3-degree-patch case. On the other hand, the line-edge velocity width still has roughly a peak value of about

50 km s^{-1}, essentially unchanged from the 3 degree patch. As such, the overall trend is now for this width to increase as one goes from line-centre to line-edge, which is now just the same qualitative trend seen in observed WPS. However, the overall quantitative level of this variation for the 1-degree-patch WPS is about a factor 3 below what is typically observed.

4.2. Location of line formation

We have also carried out simulations with different line emission region locations, to investigate whether the structure properties would evolve during their advection through the simulation grid, from the photosphere out to 10 $R_\star$. While the dynamical properties of the profile sub-peaks are indeed quite dependent on the wind location of the line emission region (Dessart & Owocki 2002b), we did not find any corresponding modification to the velocity scale σ_ξ. The increased full profile width allows more sub-peaks to appear, which merely reflects that, given the larger extent of velocity bounds of the flat top profile, more sub-peaks with their typical widths (unrelated to the terminal velocity of the wind) can fit. In this respect, the higher terminal velocity stars show profile sub-peaks suffering less degeneracy (frequency overlap), but sharing similar sub-peak velocity scales.

4.3. Instability structure with higher cutoff in line-driving opacity

Finally, we have also examined the sensitivity of these synthetic WPS properties on the details of our 1D instability simulations. We find similar results for both of the two independent hydro codes we have developed (one based on Zeus-2D developed by LD and the other based on VH-1 developed by SPO). Within each code, the inherently strong instability of line-driving leads to extensive self-excited wind structure even in the absence of any explicit perturbations from the underlying star. The overall strength of the structure can depend on certain details, most notably the spatial grid resolution and the line-opacity cutoff parameter $\kappa_{\max}/\kappa_o$. (See appendix of DO, and associated references.) For an appropriately fine spatial grid, increasing this opacity cutoff toward the most physically appropriate value $\kappa_{\max}/\kappa_o \approx 1$ leads to flow structure which, when viewed in the usual plots of velocity and density vs. height, exhibits particularly strong velocity peaks within highly rarefied flow regions. However, when plotted as velocity or density vs. a mass distribution coordinate, as in Fig. 1 here, then the effects are less dramatic, particularly for the bulk material outside the narrow velocity spikes that represents the high-speed rarefactions. Since the line-emission profile depends largely on this mass-distribution of velocity, its general properties, including the velocity scale, are not too sensitive to details like the assumed driving opacity cutoff.

5. Discussion

Previous analyses (e.g., by LM) have implicitly assumed that the finite velocity width of profile sub-peaks reflects the emitting wind structures' velocity dispersion along the relevant line of sight. This is indeed valid near the line-edges, for which the emission comes from regimes at either the extreme back or front of the emission volume, with a nearly radial sight line to the observer. But near line-centre the emission is from lobes to the side of the star, with now a nearly lateral line of sight that cuts across the flow structures, and thus is sensitive not only to any lateral velocity variation, but also to the projected change in radial velocity across the structures azimuthal extent. Thus, there arises a line-centre velocity dispersion, of order $\Delta v \approx \alpha v_r$, even when, as is the case in the synthetic models here, there is *no* lateral velocity. As such, an observed characteristic velocity width of sub-peaks near line-centre provides, given an assumed radial outflow speed of the line formation, an upper limit to the characteristic lateral spatial scale, i.e. the patch size, of the associated flow structure.

By contrast, the observed velocity widths of sub-peaks near line-edges are quite insensitive to the lateral scale size of flow structure, but provide a relatively direct diagnostic of their radial velocity dispersion. In this context, the failure of our synthetic patch models to reproduce the observed line-edge velocity widths must be viewed as a serious physical shortcoming of the assumed models.

It seems likely that a key factor in this discrepancy lies in the 1D nature of the basic hydrodynamical simulation models. In a 1D flow, there is no possibility of flow shear or vorticity, and so speed variations must necessarily have non-zero divergence, either as expansions that lead to density rarefaction, or compression that lead to density enhancement in localised clumps. Moreover, in these highly supersonic flows, the compressions necessarily reach a small spatial scale in which any internal velocity dispersion is quickly dissipated. As illustrated in Fig. 1, when a radial cut of such flow structure is viewed in terms of the velocity vs. a mass distribution, the individual density clumps thus appear as a series of near-plateaus in velocity. This associated lack of internal velocity dispersion thus seems to be at the heart of the relatively small line-edge velocity widths seen in essentially all our synthetic WPS.

A key issue this raises for future work is thus whether more realistic 2D or 3D simulation models of this intrinsic line-driven instability might yield a flow structure with a greater level of radial velocity dispersion. In considering this, an appropriate analogy may be the contrast between single-lane vs. multi-lane traffic flow. In the former, any blockage leads quickly to a compression and slow-down of traffic, with relatively little velocity variation associated with a given compression. But in the latter, a blockage in one lane has a lesser effect in other lanes, still inducing an overall slowdown in traffic, but now allowing for flow *around* the blockage that is characterised by a considerable lane-to-lane variation, or shear, in flow speed. An observer (e.g. a radar speed control) looking along the traffic would certainly detect a greater level of velocity dispersion in the latter case than the former. Translating this into the more formal language of turbulence theory, it is well known that the dimensionality considered can have a dramatic effect on the properties of the fluctuation spectrum (e.g. Mac Low et al. 1998).

A central difficulty to developing multi-dimensional structure models here arises from the non-local radiative transfer

needed to compute the line-driving force and associated instability that is the root cause of the extensive flow structure. In principle this would involve a costly computation of optical depth integrals for a suitable set of angle directions from each spatial location of the 2D or 3D structure model (Owocki 1998). On the other hand, since the radiative driving and its instability are primarily along the radial direction, a reasonable first approximation may be to simply restrict this optical depth integration to just the *radial* direction, while still allowing a multi-dimensional evolution of the hydrodynamics variables. Although this would then ignore the dynamical role of lateral line-forces, as well as the contributions of lateral variations to the radial driving, it would now allow for the essential possibility of multi-dimensional flow with non-zero lateral velocity and shear. We are currently experimenting with such radially driven, multi-dimensional simulation models, and hope to report results in a future paper.

6. Summary

We have presented a study of synthetic LPV as produced by a 3D distribution of radiative instability generated structures, following the patch method presented in DO. To allow a quantitative and objective description of the LPV characteristics, we performed a wavelet analysis of the time-dependent profile residual, providing a measure of the velocity scales of LPV at all profile locations. Observations reveal that the WPS increases from line-centre to line-edge, from ∼50 to 100–200 km s^{-1}. We suggest two distinct broadening mechanisms at the origin of this trend. At line-centre, it is due to the lateral extension of the wind blobs, possibly with additional lateral velocity. Towards line-edge, this contribution diminishes in favour of the intrinsic radial velocity dispersion of wind structures. The observed values are compatible with a lateral extension of wind blobs of ca. 3 deg, as well as the presence of a significant radial velocity dispersion intrinsic to wind structures. While the former characteristics can be easily reproduced with our patch method by modulating the patch angle, we find that our 1D radiation hydrodynamics simulations reveal wind structures with little radial velocity dispersion, i.e. ca. 50 km s^{-1}, a factor of a few smaller than observed. Attempts to resolve that discrepancy by modulating the patch size, the line emission position or the parameters governing the radiative instability failed. Interestingly, we find that while a patch size of 1 deg reproduces qualitatively the observed increasing trend of sub-peak velocity scales from line centre to edge, it leads to a significant underestimate of the observed scale at line centre.

We conjecture that the one-dimensionality of the hydrodynamical models may be a key limitation. The essential approximation of the patch method, i.e. that the wind volume can be represented as a collection of independent cones, might not necessarily be inadequate. In fact, it should hold in a global viewpoint because of the overwhelming radial driving of hot star winds which must make the correlation between wind points lying in two widely separated directions negligible. But we do anticipate that lateral pressure forces, neglected in our modelling so far, could play a subtle but key role in the overall structure. This perspective is supported by the fact that lateral communication at the sound speed leads roughly to a lateral scale size that best fits the observed fluctuation level. It suggests that the next step in modelling wind structure might focus on allowing for lateral gas pressure coupling within a multi-dimensional hydrodynamical model that is made more tractable by ignoring lateral radiation forces. We are currently exploring such an approach.

Acknowledgements. Some hydrodynamics simulations were performed on the basis of the ZEUS–2D code developed at the National Centre for Super-computing Applications (NCSA) at the University of Urbana, Illinois. LD acknowledges financial support from the University of Delaware for a visit to the Bartol Research Institute. SPO acknowledges support of NASA grant NAGW5-3530 and NSF grant AST-0097983, awarded to the University of Delaware.

References

Castor, J. I., Abbott, D. C., & Klein, R. I. 1975, ApJ, 195, 157 (CAK)
Dessart, L., & Owocki, S. P. 2002a, A&A, 383, 1113 (DO)
Dessart, L., & Owocki, S. P. 2002b, in preparation
Feldmeier, A. 1995, A&A, 299, 523
Lépine, S. 1998, Ph.D. Thesis, Université de Montréal
Lépine, S., & Moffat, A. F. J. 1999, ApJ, 514, 909 (LM)
Lépine, S., Moffat, A. F. J., & Henriksen, R. N. 1996, ApJ, 466, 392
Mac Low, M. M., Klessen, R. S., Burkert, A., & Smith, M. D. 1998, Phys. Rev. Lett., 80, 2754
Owocki, S. P., Castor, J. I., & Rybicki, G. B. 1988, ApJ, 335, 914
Owocki, S. P. 1991, in Stellar Atmospheres: Beyond Classical Models, 235
Owocki, S. P., & Puls, J. 1999, ApJ, 510, 355
Owocki, S. P. 1999, in Variable and Non-spherical Stellar Winds in Luminous Hot Stars, 294
Pauldrach, A., Puls, J., & Kudritzki, R. P. 1986, A&A, 164, 86
Robert, C. 1992, Ph.D. Thesis, Université de Montréal